

## Scaling analysis and direct simulation of unsteady natural convection cooling of fluid with $Pr < 1$ in a vertical cylinder

Wenxian Lin<sup>1,2</sup> and S. W. Armfield<sup>1</sup>

<sup>1</sup>School of Aerospace, Mechanical & Mechatronics Engineering,  
 The University of Sydney, NSW 2006, AUSTRALIA

<sup>2</sup>Solar Energy Research Institute, Yunnan Normal University,  
 Kunming, Yunnan 650092, P. R. China

### Abstract

The unsteady natural convection cooling of fluid with  $Pr < 1$  in a vertical cylinder with an imposed lower temperature on vertical sidewalls is dominated by three distinct stages of development, *i.e.* the boundary-layer development stage adjacent to the sidewall, the stratification stage, and the cooling-down stage, respectively. Various scaling laws to describe the unsteady flow behavior at these respective stages are developed with scaling analysis and are verified and quantified by direct numerical simulation with selected values of the aspect ratio of the cylinder  $A$ , the Rayleigh number  $Ra$ , and the Prandtl number  $Pr$  in the ranges of  $1/3 \leq A \leq 3$ ,  $10^6 \leq Ra \leq 10^{10}$ , and  $0.01 \leq Pr \leq 0.5$ .

### Introduction

Cooling/heating a body of fluid in an enclosure via natural convection with an imposed temperature difference or heat flux on the enclosure boundary is widely encountered in nature and in engineering settings, and the understanding of its transient flow behavior is of fundamental interest and practical importance. In the past decades, extensive experimental, numerical, and analytical studies have been conducted on this issue, although mainly on the more specific case of a rectangular cavity with differentially heated sidewalls (see, *e.g.* [1, 2]).

Patterson and Imberger [3] used a scaling analysis in their pioneering investigation of the transient behavior that occurs when the opposing two vertical sidewalls of a two-dimensional rectangular cavity are impulsively heated and cooled by an equal amount. They devised a classification of the flow development through several transient flow regimes to one of three steady-state types of flow based on the relative values of  $Ra$ ,  $Pr$ , and  $A$ . This Patterson-Imberger flow model has since occupied the center stage of research into understanding natural convection flow in cavities, and numerous investigations subsequently focused on diverse aspects of the model (see, *e.g.* [4, 5, 6, 7]).

The majority of the past studies have focused on fluids with  $Pr \geq 1$  owing to their relevance in theoretical and practical applications. Natural convection flows with  $Pr < 1$  are very important as well, in such applications as the Earth's liquid core convection, crystal growth in semiconductors, melting processes, etc., not to mention those using air and other gases as the working medium. However, studies on unsteady natural convection flows of fluids with  $Pr \ll 1$  resulting from heating/cooling vertical boundaries, together with studies on the effect of  $Pr$  variation, are scarce. This scarcity, together with the apparently incomplete understanding of  $Pr \leq 1$  flows, motivates the current study.

### Scaling Analysis

Under consideration is the flow behavior of cooling a quiescent isothermal Newtonian fluid with  $Pr < 1$  in a vertical cylinder by unsteady natural convection due to an imposed fixed lower

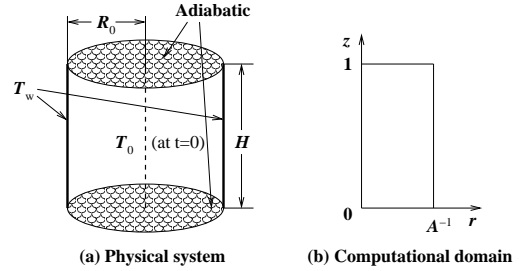


Figure 1: A sketch of the physical system considered and the computational domain used for numerical simulations.

temperature on the vertical sidewalls. The cylinder has a height of  $H$  and a radius of  $R_0$ , as sketched in Fig. 1. It is assumed that the fluid cooling is the result of the imposed fixed temperature  $T_w$  on the vertical sidewalls while all the remaining boundaries are adiabatic and all boundaries are non-slip, and the fluid in the cylinder is initially at rest and at a uniform temperature  $T_0$  ( $T_0 > T_w$ ). It is also assumed that the flows are laminar.

The governing equations of motion are the Navier-Stokes equations with the Boussinesq approximation for buoyancy, which together with the temperature transport equation can be written in the following two-dimensional form,

$$\frac{1}{R} \frac{\partial(RU)}{\partial R} + \frac{\partial V}{\partial Z} = 0, \quad (1)$$

$$\begin{aligned} \frac{\partial U}{\partial t} + \frac{1}{R} \frac{\partial(RUU)}{\partial R} + \frac{\partial(VU)}{\partial Z} = -\frac{1}{\rho} \frac{\partial P}{\partial R} \\ + \nu \left\{ \frac{\partial}{\partial R} \left[ \frac{1}{R} \frac{\partial(RU)}{\partial R} \right] + \frac{\partial^2 U}{\partial Z^2} \right\}, \end{aligned} \quad (2)$$

$$\begin{aligned} \frac{\partial V}{\partial t} + \frac{1}{R} \frac{\partial(RUV)}{\partial R} + \frac{\partial(VV)}{\partial Z} = -\frac{1}{\rho} \frac{\partial P}{\partial Z} \\ + \nu \left[ \frac{1}{R} \frac{\partial}{\partial R} \left( R \frac{\partial V}{\partial R} \right) + \frac{\partial^2 V}{\partial Z^2} \right] + g\beta(T - T_0), \end{aligned} \quad (3)$$

$$\frac{\partial T}{\partial t} + \frac{1}{R} \frac{\partial(RUT)}{\partial R} + \frac{\partial(VT)}{\partial Z} = \kappa \left[ \frac{1}{R} \frac{\partial}{\partial R} \left( R \frac{\partial T}{\partial R} \right) + \frac{\partial^2 T}{\partial Z^2} \right], \quad (4)$$

where  $U$  and  $V$  are the radial ( $R$ -direction) and vertical ( $Z$ -direction) velocity components,  $t$  is the time,  $P$  is the pressure,  $T$  is the temperature,  $g$  is the acceleration due to gravity,  $\beta$ ,  $\nu$  and  $\kappa$  are the thermal expansion coefficient, kinematic viscosity and thermal diffusivity of the fluid, respectively. The gravity acts in the negative  $Z$ -direction.

The flow considered here is dominated by three distinct stages of development, *i.e.* the boundary-layer development stage, the

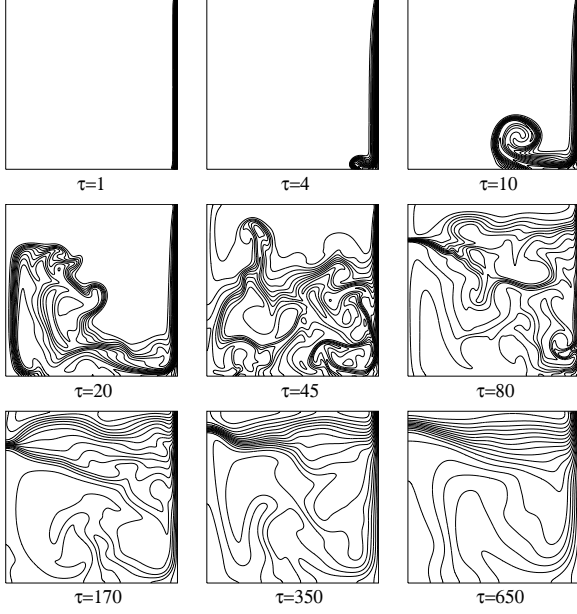


Figure 2: Numerically simulated temperature contours at the stages of the boundary-layer development (top row), the stratification (middle row), and the cooling-down (bottom row), respectively, for  $Ra = 10^8$ ,  $A = 1$ , and  $Pr = 0.1$ .

stratification stage, and the cooling-down stage, respectively, as illustrated in Fig. 2, where numerically simulated temperature contours are shown for the three stages for the specific case of  $Ra = 10^8$ ,  $Pr = 0.1$  and  $A = 1$ , where  $Ra$ ,  $Pr$  and  $A$  are defined as

$$Ra = \frac{g\beta(T_0 - T_w)H^3}{\nu\kappa}, \quad Pr = \frac{\nu}{\kappa}, \quad A = \frac{H}{R_0}.$$

In this case the boundary-layer development is seen in the temperature contours adjacent to the righthand, cooled, wall, with the boundary-layer development completed by around  $\tau = 10$ , where  $\tau$  is the dimensionless time, made dimensionless by  $H^2/(\kappa Ra^{1/2})$ . The cooled fluid ejected by the boundary layer acts to fill and stratify the domain, seen in the stratification stage, from  $\tau = 20$  to 80. Finally the stratification is gradually reduced in the cooling-down stage of the flow, for  $\tau > 170$ . In this section, scaling relations will be developed for the relevant parameters characterizing the flow behavior at these respective stages of flow development.

The vertical boundary layer adjacent to the cooled sidewall experiences a start-up stage, followed by a short transitional stage before reaching a steady-state stage. The parameters characterizing the flow behavior at this development stage are the thermal boundary-layer thickness  $\Delta_T$ , the maximum vertical velocity  $V_m$ , the time  $t_s$  for the boundary-layer development to reach the steady state, and the Nusselt number  $Nu$  across the sidewall.

Heat is initially transferred out through the vertical wall from the fluid by conduction after the initiation of the flow, resulting in a vertical thermal boundary layer of thickness  $O(\Delta_T)$  adjacent to the wall, where at height  $Z$ , from Eq. (4), the balance between the inertial term  $O([T_0 - T_w]/t)$  and the conductive term  $O(\kappa[T_0 - T_w]/\Delta_T^2)$  dominates the flow, which gives,

$$\Delta_T \sim \kappa^{1/2} t^{1/2}, \quad (5)$$

or, in dimensionless form,

$$\delta_T = \frac{\Delta_T}{H} \sim Ra^{-1/4} \tau^{1/2}, \quad (6)$$

in which “ $\sim$ ” means “scales with” and  $\tau = t/(H/V_0)$  is the dimensionless time, where  $V_0 = \kappa Ra^{1/2}/H$  is the characteristic velocity scale. During this start-up stage, the dominant balance in Eq. (3) for  $Pr < 1$  is that between the inertia force  $O(V_m/t)$  and the buoyant force  $O(g\beta[T_0 - T_w])$ , which gives

$$V_m \sim g\beta(T_0 - T_w)t \sim \frac{Ra\nu\kappa}{H^3}t, \quad (7)$$

or, in dimensionless form,

$$v_m = \frac{V_m}{V_0} \sim Pr\tau, \quad (8)$$

After the start-up stage, the dominant balance at height  $Z$  in Eq. (4) gradually shifts from that between the inertial term  $O([T_0 - T_w]/t)$  and the conductive term  $O(\kappa[T_0 - T_w]/\Delta_T^2)$  to that between the inertial term and the convective term  $O(V_m[T_0 - T_w]/[H - Z])$ , until the latter balance becomes fully dominant and the thermal boundary-layer development then reaches its steady-state stage. The inertia-convective balance in Eq. (4) gives

$$\frac{T_0 - T_w}{t} \sim \frac{V_m[T_0 - T_w]}{H - Z}. \quad (9)$$

Using Eqs. (5) and (7), this leads to

$$t_b \sim \left[ \frac{H - Z}{g\beta(T_0 - T_w)} \right]^{1/2} \sim \frac{H^2}{\kappa Ra^{1/2} Pr^{1/2}} \left( 1 - \frac{Z}{H} \right)^{1/2}, \quad (10)$$

or, in dimensionless form,

$$\tau_b = \frac{t_b}{(H/V_0)} \sim \left( \frac{1 - z}{Pr} \right)^{1/2}, \quad (11)$$

which represents the local time scale for the thermal boundary layer at height  $Z$  to reach the steady state, where  $z = Z/H$  is the dimensionless vertical coordinate.

At time  $t_b$ , the thermal boundary layer at height  $Z$  reaches its steady-state thickness scale  $\Delta_{T,b}$ , which, from Eq. (5), is as follows,

$$\Delta_{T,b} \sim \kappa^{1/2} \left[ \frac{H - Z}{g\beta(T_0 - T_w)} \right]^{1/4} \sim \frac{H^{3/4}(H - Z)^{1/4}}{Ra^{1/4} Pr^{1/4}}, \quad (12)$$

or, in dimensionless form,

$$\delta_{T,b} = \frac{\Delta_{T,b}}{H} \sim \left( \frac{1 - z}{Pr Ra} \right)^{1/4}, \quad (13)$$

and the steady-state vertical velocity scale  $V_{m,b}$  at height  $Z$  within this thermal boundary layer is, from Eq. (7), as follows,

$$V_{m,b} \sim \frac{\kappa Ra^{1/2} Pr^{1/2}}{H} \left( 1 - \frac{Z}{H} \right)^{1/2}, \quad (14)$$

or, in dimensionless form,

$$v_{m,b} = \frac{V_{m,b}}{V_0} \sim [(1 - z)Pr]^{1/2}. \quad (15)$$

The heat transfer across the vertical sidewall is represented by the following local Nusselt number  $Nu$  at height  $Z$ ,

$$Nu \sim \left[ \frac{R_0}{(T_0 - T_w)} \frac{\partial T}{\partial R} \right]_{R=R_0}. \quad (16)$$

Therefore, during the start-up stage,

$$Nu \sim \frac{R_0}{\Delta_T} \sim \frac{R_0}{\kappa^{1/2} t^{1/2}} \sim \frac{1}{A} Ra^{1/4} \tau^{-1/2}, \quad (17)$$

and at the steady-state stage,

$$Nu_b \sim \frac{R_0}{\Delta_{T,b}} \sim \frac{(PrRa)^{1/4}}{A(1-Z/H)^{1/4}} \sim \frac{1}{A} \left( \frac{PrRa}{1-z} \right)^{1/4}, \quad (18)$$

Equations (6), (8), and (17) clearly show that during the start-up stage, the boundary-layer development on the vertical sidewalls is independent of  $z$ , however, as shown by (13), (15), and (18), the boundary-layer development and the heat transfer across the vertical sidewall become  $z$  dependent at the steady-state stage of the boundary-layer development.

Once the boundary layer is fully developed, the fluid in the cylinder is gradually stratified by the cooled fluid ejected from the boundary layer, starting from the bottom of the cylinder. The time  $t_s$  for the full stratification of the whole fluid in the cylinder will be at the moment when the volume of the cooled fluid ejected from the boundary layer is equal to the volume of the cylinder. The rate of flow of fluid through the boundary layer is characterized by  $\Delta_{T,b} V_{m,b}$ , and therefore the time to full stratification is characterized by

$$t_s \sim \frac{HR_0}{\kappa Ra^{1/2}} \left( \frac{Ra}{Pr} \right)^{1/4}, \quad (19)$$

which is in dimensionless form as follows,

$$\tau_s = \frac{t_s}{(H/V_0)} \sim \frac{1}{A} \left( \frac{Ra}{Pr} \right)^{1/4}. \quad (20)$$

After the full stratification, the fluid in the cylinder is continually cooled down until the whole body of fluid has the same temperature as that imposed on the sidewalls. The appropriate parameters to characterize this cooling-down process are the time  $t_f$  for the fluid to be fully cooled down, the average fluid temperature  $T_a(t)$  over the whole volume of the cylinder at time  $t$ , and the average Nusselt number on the cooling wall.

As the fluid cooling-down is achieved by maintaining a fixed temperature  $T_w$  on the vertical sidewalls while keeping the top and bottom boundaries adiabatic, all the heat used to fully cool down the fluid in the cylinder must pass through the sidewalls, and then energy conservation in the cylinder requires that,

$$\rho c_p V_c (T_0 - T_w) \sim t_f A_s k \frac{(T_0 - T_w)}{\bar{\Delta}_{T,b}}, \quad (21)$$

where  $V_c = \pi R_0^2 H$  is the volume of the fluid in the cylinder,  $A_s = 2\pi R_0 H$  is the surface area of the sidewall,  $k$  is the thermal conductivity of fluid, and  $\bar{\Delta}_{T,b}$  is the average thermal boundary-layer thickness which is calculated as follows,

$$\bar{\Delta}_{T,b} = \frac{1}{H} \int_0^H \Delta_{T,b} dZ. \quad (22)$$

Therefore,  $t_f$  has the following scaling relation,

$$t_f \sim \frac{R_0 \bar{\Delta}_{T,b}}{\kappa} \sim \frac{R_0 H}{\kappa (PrRa)^{1/4}}, \quad (23)$$

where  $\kappa = k/(\rho c_p)$ , which is in dimensionless form as follows,

$$\tau_f = \frac{t_f}{(H/V_0)} \sim \frac{1}{A} \left( \frac{Ra}{Pr} \right)^{1/4}. \quad (24)$$

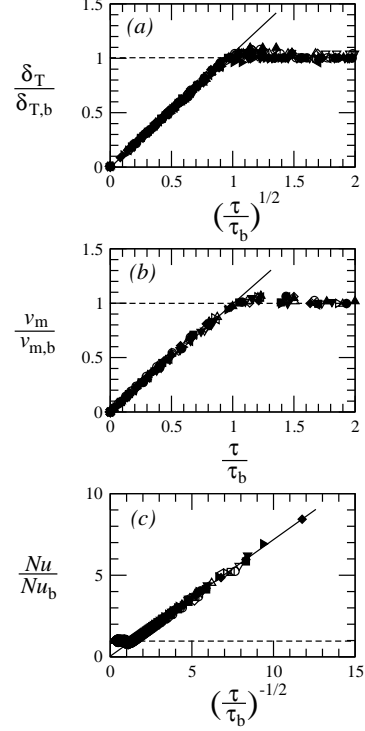


Figure 3: Numerical results for (a)  $\delta_T/\delta_{T,b}$  plotted against  $(\tau/\tau_b)^{1/2}$ ; (b)  $v_m/v_{m,b}$  plotted against  $\tau/\tau_b$ ; and (c)  $Nu/Nu_b$  plotted against  $(\tau/\tau_b)^{-1/2}$ . solid line, linear fit for the start-up stage; dashed line, linear fit for the steady-state stage.

The decay of the average fluid temperature  $T_a(t)$  is expected to obey an exponential relation[8], that is,

$$\frac{T_a(t) - T_0}{T_0 - T_w} = e^{-f(Ra, Pr, A)t} - 1, \quad (25)$$

where  $f(Ra, Pr, A)$  is some function of  $Ra$ ,  $Pr$ , and  $A$ , which is in dimensionless form as follows

$$\theta_a(\tau) = e^{-C_f A \left( \frac{Pr}{Ra} \right)^{1/4} \tau} - 1, \quad (26)$$

where  $C_f$  is a constant of proportionality which will be determined below by numerical results.

### Numerical results

In this section, the scaling relations obtained above will be validated and quantified by a series of direct numerical simulations with selected values of  $A$ ,  $Ra$ , and  $Pr$  in the ranges of  $1/3 \leq A \leq 3$ ,  $10^6 \leq Ra \leq 10^{10}$ , and  $0.01 \leq Pr \leq 0.5$ . A total of 12 simulation runs have been carried out for this purpose. Specifically, results have been obtained with  $Ra = 10^6, 10^7, 10^8, 10^9$ , and  $10^{10}$ , while keeping  $A = 1$  and  $Pr = 0.1$  unchanged, to show the dependence of the scaling relations on  $Ra$  (Runs 1-5); the runs with  $A = 1/3, 1/2, 1, 2$ , and  $3$ , while keeping  $Ra = 10^8$  and  $Pr = 0.1$  unchanged, have been carried out to show the dependence on  $A$  (Runs 6-7, 3, and 8-9); and the runs with  $Pr = 0.01, 0.05, 0.1$ , and  $0.5$ , while keeping  $Ra = 10^8$  and  $A = 1$  unchanged, have been carried out to show the dependence on  $Pr$  (Runs 10-11, 3, and 12), respectively.

Detailed information about the numerical algorithm, mesh construction, initial and boundary conditions, and numerical accuracy tests can be found in [5, 6].

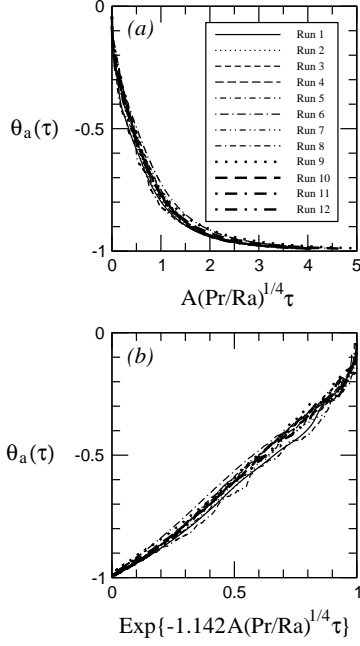


Figure 4: Numerical results for  $\theta_a(\tau)$  plotted against (a)  $A(Pr/Ra)^{1/4}\tau$  and (b)  $e^{-1.142A(Pr/Ra)^{1/4}\tau}$  for all simulation runs.

The numerical results for  $\delta_T$ ,  $v_m$ , and  $Nu$  at the boundary-layer development stage are plotted as a ratio with respect to their steady-state values against the scaled times  $\tau/\tau_b$  in Fig. 3. The results for  $\tau/\tau_b < 1$  fall onto a straight line, confirming the scaling laws at the start-up stage, while the results for  $\tau/\tau_b \geq 1$  fall onto a horizontal line, confirming the scaling laws at the steady-state stage. The numerically quantified scaling laws are therefore as follows,

$$\tau_b = 2.395 \left( \frac{1-z}{Pr} \right)^{1/2}, \quad (27)$$

$$\delta_{T,b} = 4.845 \left( \frac{1-z}{PrRa} \right)^{1/4}, \quad (28)$$

$$v_{m,b} = 0.872[(1-z)Pr]^{1/2}, \quad (29)$$

$$Nu_b = \frac{0.519}{A} \left( \frac{PrRa}{1-z} \right)^{1/4}, \quad (30)$$

$$\overline{Nu}_b = \frac{0.658}{A} (PrRa)^{1/4}. \quad (31)$$

$$\delta_T = 3.131Ra^{-1/4}\tau^{1/2}, \quad (32)$$

$$v_m = 0.364Pr\tau, \quad (33)$$

$$Nu = \frac{0.803}{A} Ra^{1/4}\tau^{-1/2}, \quad (34)$$

$$\overline{Nu} = \frac{1.018}{A} Ra^{1/4}\tau^{-1/2}. \quad (35)$$

The numerical results show that  $\tau_s$  can be well approximated by the following expression

$$\tau_s = \frac{0.313}{A} \left( \frac{Ra}{Pr} \right)^{1/4}. \quad (36)$$

which clearly demonstrate that the scaling law (20) is correct for the stratification stage.

The numerical results also show that  $\tau_f$  can be well approxi-

mated by the following expression

$$\tau_f = \frac{4.031}{A} \left( \frac{Ra}{Pr} \right)^{1/4}, \quad (37)$$

where  $\tau_f$  was determined as the time at which  $\theta_a(\tau_f) = -0.99$ , which clearly demonstrate that the scaling law (24) is correct for the cooling-down stage. Therefore, the full expression for the time decay of  $\theta_a$ , Eq. (26), is obtained as

$$\theta_a(\tau) = e^{-1.142A \left( \frac{Pr}{Ra} \right)^{1/4} \tau} - 1. \quad (38)$$

The numerical results presented in Fig. 4 show that all sets of data fall onto a single curve, indicating that the scaling relation (26) is correct.

## Conclusions

The cooling down behavior of a fluid contained in a vertical cylinder subjected to isothermal boundary condition on the vertical walls is examined via scaling analysis and direct numerical simulation. Scaling laws have been obtained for the development time and properties of the initial vertical thermal boundary layer, of the stratification time and of the full cooling down time. The scalings have been obtained for  $Pr < 1$ , yielding different relations from those obtained for  $Pr > 1$ . For instance the scaling relations for the time development of the boundary layer, stratification and full cooling down stages are  $\tau_b \sim (1-z)^{1/2}Pr^{-1/2}$ ,  $\tau_s \sim Ra^{1/4}Pr^{-1/4}/A$ ,  $\tau_f \sim Ra^{1/4}Pr^{-1/4}/A$  respectively for  $Pr < 1$ , and  $\tau_b \sim (1-z)^{1/2}$ ,  $\tau_s \sim Ra^{1/4}/A$ ,  $\tau_f \sim Ra^{1/4}/A$  respectively for  $Pr > 1$  [6]. It is seen that for  $Pr > 1$  the scaled quantities are independent of  $Pr$ , while for  $Pr < 1$  they show a  $Pr$  dependency.

## Acknowledgements

The financial support of the Australian Research Council, via an Australian Postdoctoral Fellowship (Grant No. DP0449876), the National Natural Science Foundation of China (Grant No. 10262003), and the Natural Science Foundation of Yunnan Province of China (Key Project, Grant No. 2003E0004Z) are gratefully acknowledged.

## References

- [1] Gebhart, B., Jaluria, Y., Mahajan, R.L. and Sammakia, B., *Buoyancy-Induced Flows and Transport*, Hemisphere, 1988.
- [2] Hyun, J.M., Unsteady bouyant convection in an enclosure, *Adv. Heat Transfer*, **24**, 1994, 277–320.
- [3] Patterson, J.C. and Imberger, J., Unsteady natural convection in a rectangular cavity, *J. Fluid Mech.*, **100**, 1980, 65–86.
- [4] Bejan, A., *Convection Heat Transfer* (2nd Edn.), John Wiley & Sons, 1995.
- [5] Lin, W. and Armfield, S.W., Direct simulation of natural convection cooling in a vertical circular cylinder, *Int. J. Heat Mass Transfer*, 1999, **42**, 4117–4130.
- [6] Lin, W. and Armfield, S.W., Natural convection cooling of rectangular and cylindrical containers, *Int. J. Heat Fluid Flow*, **22**, 2001, 72–81.
- [7] Lin, W. and Armfield, S.W., Long-term behavior of cooling fluid in a rectangular container, *Phys. Rev. E*, **69**, 2004, 056315.
- [8] Mills, A.F., *Heat Transfer* (2nd Edn.), Prentice Hall, 1999.